



Contents lists available at ScienceDirect

Biochemical and Biophysical Research Communications

journal homepage: www.elsevier.com/locate/ybbrc



Identification of a new membrane-permeable inhibitor against inositol-1,4,5-trisphosphate-3-kinase A



Dominik Schröder^a, Christoph Rehbach^a, Carola Seyffarth^b, Martin Neuenschwander^b, Jens V. Kries^b, Sabine Windhorst^{a,*}

^a Institut für Biochemie und Signaltransduktion, UKE Hamburg, Martinistr. 52, 20246 Hamburg, Germany

^b Screening Unit, FMB Berlin, Robert-Rössle-Str. 10, 10355 Berlin, Germany

ARTICLE INFO

Article history:

Received 13 August 2013

Available online 24 August 2013

Keywords:

Metastasis

High-throughput screening

ITPKA

InsP₃

Cellular uptake

Mixed inhibition type

ITPKA-inhibitor

ABSTRACT

Ectopic expression of the neuron-specific inositol-1,4,5-trisphosphate-3-kinase A (ITPKA) in lung cancer cells increases their metastatic potential because the protein exhibits two actin regulating activities; it bundles actin filaments and regulates inositol-1,4,5-trisphosphate (InsP₃)-mediated calcium signals by phosphorylating InsP₃. Thus, in order to inhibit the metastasis-promoting activity of ITPKA, both its actin bundling and its InsP₃kinase activity has to be blocked. In this study, we performed a high throughput screen in order to identify specific and membrane-permeable substances against the InsP₃kinase activity. Among 341,44 small molecules, 237 compounds (0.7%) were identified as potential InsP₃kinase inhibitors. After determination of IC₅₀-values, the three compounds with highest specificity and highest hydrophobicity (EPPC-3, BAMB-4, MEPTT-3) were further characterized. Only BAMB-4 was nearly completely taken up by H1299 cells and remained stable after cellular uptake, thus exhibiting a robust stability and a high membrane permeability. Determination of the inhibitor type revealed that BAMB-4 belongs to the group of mixed type inhibitors. Taken together, for the first time we identified a highly membrane-permeable inhibitor against the InsP₃kinase activity of ITPKA providing the possibility to partly inhibit the metastasis-promoting effect of ITPKA in lung tumor cells.

© 2013 Elsevier Inc. All rights reserved.

1. Introduction

Cancer is a leading cause of death worldwide [1], and most patients die from distant metastasis [2]. To develop metastasis, the cancer cells escape from the primary tumor and adhere to and invade the extracellular matrix. In a next step, the cells migrate through the connective tissue, intravasate into and extravasate from blood vessels to establish distant metastasis [2]. During this process a dynamic remodelling of the actin cytoskeleton occurs, which is regulated by the activity of actin binding proteins (ABP). Based on the essential role of ABPs for regulation of actin dynamics, many ABPs are essential for cancer cell metastasis (summarized in [3]). Our group identified inositol-1,4,5-trisphosphate-3-kinase A (ITPKA) as an ABP essential for metastasis of lung cancer cells and showed that its expression is up-regulated in tumor samples from lung cancer patients [4,5].

ITPKA forms homodimers and binds actin filaments by its N-terminal domain (aa 1–52), leading to bundling of actin filaments

[4,6]. This actin bundling activity of ITPKA is necessary for formation of filopodia, lamellipodia and invadopodia in ITPKA expressing tumor cells [4,5]. Since these protrusions are required for tumor cells to adhere to the substrate, to move forward and to transigrate through the endothelial cell layer [7] expression of ITPKA is essential for lung cancer metastasis [4]. In addition to its actin bundling activity, ITPKA phosphorylates the calcium mobilizing second messenger inositol-1,4,5-trisphosphate (InsP₃) at position three, thus is essential for regulation of InsP₃-mediated calcium signals [4]. Calcium signals regulate multiple cellular functions, including the process of migration; Ca²⁺/calmodulin stimulates the activity of myosin-light chain kinase, an enzyme essential for contraction of actin-myosin filaments during migration [8,9]. In addition, increased intracellular Ca²⁺ concentrations activate the actin severing activity of gelsolin, an ABP which promotes actin turnover [10].

Thus, in order to inhibit the effect of ITPKA on metastasis it is necessary to block both, its actin bundling and its InsP₃-kinase activity. Since in contrast to many ubiquitously expressed ABPs, under physiological conditions ITPKA is only expressed in brain [11,12], the protein is a very interesting target for cancer therapy. Although potent inhibitors against the InsP₃kinase activity of ITPKA have been identified [13,14] these compounds inhibit

* Corresponding author. Fax: +49 040 7410 56818.

E-mail addresses: s.windhorst@uke.de, s.windhorst@uke.uni-hamburg.de (S. Windhorst).

multiple cellular targets (summarized in [13]) as they belong to the group of plant polyphenols [13]. Furthermore, ITPKA inhibitors have been identified which solely compete for ATP, thus targeting multiple protein kinases with conserved DFG motifs [14,15]. In addition, the polyphenolic ITPKA inhibitors are only weakly membrane permeable (own unpublished data and [16]). Therefore, in this study we screened for more specific and membrane-permeable ITPKA inhibitors by High Throughput Screening (HTS).

2. Material and methods

2.1. Recombinant expression and purification of ITPKA

A C-terminal sequence of 306 amino acids containing the catalytic and CaM-domain of ITPKA was cloned into the vector pET17b and was recombinantly expressed in *Escherichia coli* BL21. The protein was enriched by phosphocellulose chromatography and purified by CaM-Sepharose affinity chromatography as described in [17].

2.2. High Throughput Screen for *InsP₃* kinase-inhibitors by using the ADP Glo Assay

The primary screen for *InsP₃* kinase-inhibitors was performed in the Screening Unit of Max-Delbrück-Centrum für Molekulare Medizin Berlin-Buch (MDC); Leibniz-Institut für Molekulare Pharmakologie im Forschungsverbund Berlin e.V. (FMP). The compounds were mainly purchased from ChemBionet (<http://www.chembionet.info/>). In addition, compounds kindly provided by different research groups were screened.

The Kinase ADP-Glo Assay was purchased from Promega, containing ADP-Glo reagent, kinase detection reagent, Ultra Pure ATP and ADP, and was adapted for use in HTS with 384 well plates. The ADP-Glo assay measures *InsP₃* kinase activity indirectly via ATP consumption. As a first step after kinase reaction not metabolized ATP is degraded. Then, the newly generated ADP is transformed back to ATP, which serves as substrate for luciferase [18,19]. Thus, the luminescent signal is proportional to ATP catalyzed by *InsP₃* kinase and correlates with kinase activity [20]. HTS was performed with Freedom Evo (Tecan) and Biomek Fx (Beckmann) robots.

For HTS screens the compounds were diluted in Dimethylsulfoxid (DMSO, Merck) and a final compound concentration of 20 μ M (9 nL) was applied to each well. As control the *InsP₃* kinase-inhibitor quercetin was used [13]. In the last 2 lines of every plate the negative (Aqua dest. and enzyme solution without ITPKA) and positive control (enzyme solution with ITPKA and without compounds) were placed. In each well 3 μ L of the enzyme solution (20 mM HEPES pH 7.5, 5 mM $MgCl_2$, 30 mM KCl, 1 mM DTT, 0.1 mM ATP, 40 nM ITPKA (0.1 μ L)) was applied. After incubation for 10 min 2 μ L *InsP₃* (125 μ M) was added and incubation was continued for 30 min at RT. Now 5 μ L of ADP-Glo reagent was added (converting remaining ADP to ATP). After incubation for 40 min at RT 10 μ L kinase detection reagent (containing luciferase which uses ATP as substrate) was added and incubation was continued for 30 min at RT. For luminescent measurements a Safire 2 (Tecan) reader was used at 400 nm with an integration time of 40 ms at a temperature of 30 °C.

In the validation screen IC_{50} values of compounds with inhibitory potential were analyzed by a serial dilution of 1:2. The concentration of the compounds at the beginning was 40 μ M and 8 dilution steps were performed in duplicates. As a control quercetin was used in the same concentration range [see 13]. We did not detect any plate or position effects.

2.3. Data Analysis and Hit Scoring

The instrument raw data (the luminescence data from the Tecan Safire 2 reader) of the high throughput screen were analyzed by Pipeline Pilot software. For each plate, the data were grouped into samples (columns 1–22 containing the compound samples), positive controls (column 23, complete reaction mixture with DMSO) and negative controls (column 24, reaction mixture without enzymes, according to no signal). For each group, the median, median absolute deviation, standard deviation and relative activity (medians of positive control were used as reference points with 1 and the medians of the negative controls were used with 0, respectively) was calculated. The median was used as robust estimation of the mean value, the median absolute deviation multiplied with the correction factor 1.4826 was used as robust estimate of the standard deviation [21].

The z-score (Z_i) (the number of standard deviations from the mean) is frequently used to normalize assay data in a way that provides explicit information about the assay quality and was calculated as:

$$Z_i = \frac{x_i - \bar{x}}{S_x}$$

where \bar{x} is the sample median and S_x is the standard deviation. The z-score implicates the distance of a sample point from the mean in reference to the standard deviation.

The screening window coefficient (z-factor) is defined as the ratio of the separation band to the dynamic range of the assay and is expressed by the formula below [22], where μ is denoted for the means of positive control signal (μ_{c+}) and negative control signal (μ_{c-}) and σ is denoted for the standard deviation of positive control signal (σ_{s+}) or negative control signal (σ_{c-}), respectively:

$$Z = \frac{|(\mu_{0+}) - (\mu_{0-})| - ((3\sigma_{0+}) + (3\sigma_{0-}))}{|(\mu_{c+}) - (\mu_{c-})|}$$

Or upon rearrangement,

Z-factor defines a characteristic parameter of the capability of hit identification for each given assay at the defined screening condition. A z-factor above 0.5 implicates a sufficient large separation band and a screening-appropriate assay [22]. The relative enzyme activity, which results from compound inhibitory activity, was calculated as follows:

$$\text{rel. activi} = \frac{x_i - \text{Median_neg_Co}}{|\text{Median_pos_Co} - \text{Median_neg_Co}|}$$

The Hit Scoring was made according to the z-score and the relative enzyme activity.

2.4. Coupled PK/LDH assay

The coupled PK/LDH optical assay was used as orthogonal assay to validate the data obtained by the ADP-Glo Assay and to determine Michaelis–Menten dissociation constants (K_m) and the maximum enzyme velocity (V_{max}). Measurements were performed as described in [13].

2.5. Determination of K_m and V_{max}

K_m for ATP was analyzed at varying ATP concentrations of 10, 50, 250 and 500 μ M and at a constant *InsP₃* concentration of 25 μ M. K_m for *InsP₃* was analyzed at 10, 25, 50 and 100 μ M *InsP₃* and at constant ATP concentration (500 μ M). For each measurement three different inhibitor concentrations (10, 20 and 40 μ M) were applied. K_m and V_{max} were evaluated by Graph Pad Prism.

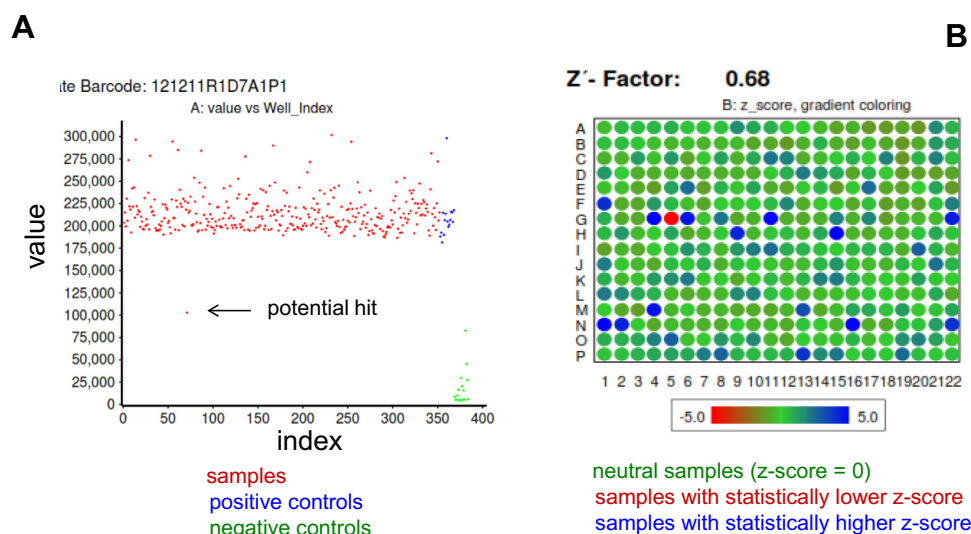


Fig. 1. Validation screen of HTS for InsP₃ kinase inhibitors. Validation of compounds identified by the primary screen was performed by determining IC₅₀ values in serial dilutions starting with 40 μ M in 9 dilution steps in duplicates using the ADP-Glo assay. The result of one randomly chosen plate is shown. (A) Raw data (value) against well index (index). (B) Z-score heat map with gradient colouring.

Table 1

Top 10 list of compounds with corresponding IC₅₀ values. On the left column the position on the 384 well plates during the tests is shown (K2 to O21). Substances marked with asterisks were selected for detailed characterization. IC₅₀ determination was performed via ADP-Glo Assay in three different experiments. Mean \pm SD is shown. Percent of inhibition of further targets analyzed in the screening unit (40–100) are given and was denoted as % inhibition frequency.

Compound	IC ₅₀ (μ M)	Inhibition frequency (%)
K2	36 \pm 5	44
K4	16 \pm 11	30
M10*	17 \pm 8	8
M11	19 \pm 11	63
O12*	36 \pm 4	12
I15	31 \pm 11	15
C14*	37 \pm 13	2.4
G17	24 \pm 5	46
K21	27 \pm 3	45
O21	38 \pm 3	42

The inhibition mechanism was determined by Lineweaver Burk- and Dixon-Plots.

2.6. Determination of cellular uptake by HPLC

H1299 cells were cultured in 5 ml DMEM-Medium/10% fetal calf serum to about 90% confluence and were incubated with 100 μ M inhibitor for 24 h. For every experiment a control dish remained untreated to serve as deficiency control. After washing the cells fivefold with phosphate saline (PBS), the cells were treated with 2 ml trypsin, centrifuged (5 min; 1600 rpm; 4 $^{\circ}$ C), and washed with PBS. Supernatants were decanted and 200 μ l methanol was added to extract the inhibitors. For deficiency controls 100 μ M of the inhibitor was added to trypsinized, untreated cells. Tubes were incubated for 5 min on the plate shaker (Heidolph, Duomax 1030) and centrifuged for 10 min at 13 000 rpm at 4 $^{\circ}$ C. Supernatants were collected and the methanol extraction was repeated twice. The 3 fractions were combined and dried via speed Vac (Christ, Alpha RVC). The lyophilisates were resuspended in 200 μ l DMSO.

The concentration of extracted inhibitors was analyzed by HPLC (Varian Pro Star Model 210). A C4 pre-column from Supelco (Cat# 59592) and, depending on the inhibitor, a C4-column (Supelcosil LC 304, Cat# 58824) or a C18 column (Supelco Discovery C18,

Cat# 504971) was used for separation. HPLC analysis was performed with a flow rate of 1 ml/min at 22 $^{\circ}$ C. For each separation an injection volume of 500 μ l (200 μ l sample and 300 μ l buffer A, see results) was used. Methanol, acetonitrile and sodium dihydrogen phosphate (NaH₂PO₄) were purchased from Merck (LiChrosolv). H₂O dest. and buffers for HPLC were sterile filtered.

2.7. Statistics

Significances were analyzed by One Way ANOVA with Graph Pad Prism.

3. Results and discussion

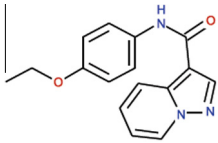
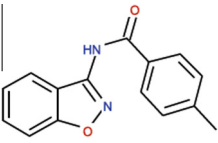
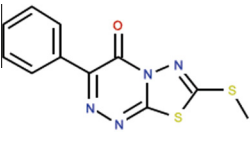
3.1. Primary screen for ITPKA inhibitors and revalidation

In order to identify specific and membrane-permeable ITPKA inhibitors, a high-throughput screen of 341,44 chemical compounds was performed. In general, the coupled PK/LDH optical assay was used to measure InsP₃ kinase activity [e.g. 13]. However, since it was not possible to adapt this assay to HTS, the compound screen was performed with the ADP-Glo assay (for details, see methods).

To identify valid measurements, the median activity and z-score (for details, see methods) were plotted for each measurement per 384 well plates. The mean z-factor for all 97 plates was 0.82 ± 0.079 , which was accepted because z-factors above 0.5 represent valid measurements [22]. 237 Compounds were identified in the primary screen with a potential inhibitory effect (data not shown). This hit rate of 0.7% is in accordance with published data [e.g. 18, 19]. The 237 primary hits were validated by determining IC₅₀ values. A serial dilution of 1:2 starting with a compound concentration of 40 μ M down to 0.3 μ M (Fig. 1), in nine dilution steps in duplicates was performed. Based in this determination, we selected the 10 compounds with the lowest IC₅₀ value for manual revalidation (Table 1 and Suppl. Fig. 1). From these ten compounds, three substances with highest specificity (inhibition frequency) and best potential membrane permeability (hydrophobicity) were selected: M10, O12 and C14. Their chemical structures, structural names, given abbreviations, well positions in the screen and inhibition frequency of InsP₃ kinase activity is given in Table 2. To

Table 2

Chemical structure and names of the three selected compounds for revalidation.

Abbreviation	EPPC-3	BAMB-4	MEPTT-3
Well position	M10	C14	O12
Structural name	<i>N</i> -(4-ethoxyphenyl)pyrazolo[1,5- <i>a</i>]pyridine-3-carboxamide	<i>N</i> -(1,2-benzoxazol-3-yl)-4-methylbenzamide	7-methylsulfanyl-3-phenyl-[1,3,4]thiadiazolo[2,3- <i>c</i>][1,2,4]triazin-4-one
Chemical structure			
Inhibition at 40 μ M	87%	68%	55%

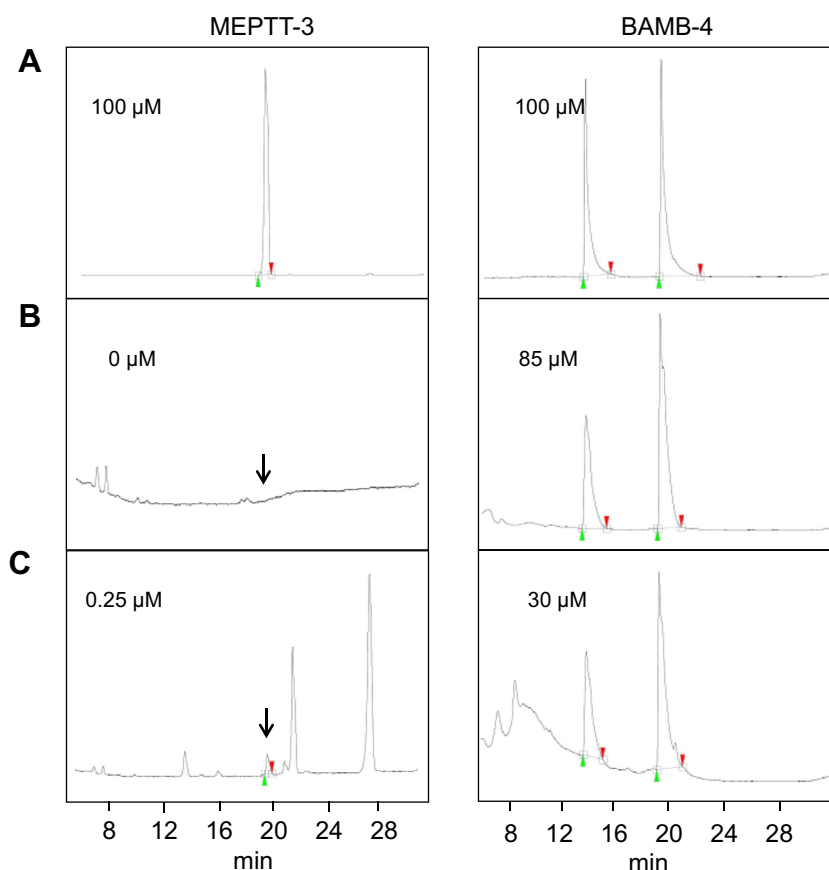


Fig. 2. Cellular uptake of InsP_3 kinase inhibitors. Cells were incubated with 100 μM Inhibitor (MEPTT-3 or BAMB-4) over night or remained untreated. Immediately to methanol extraction, 100 μM of each compound was added to untreated cells as deficiency control. Compounds were extracted by methanol and their concentration analyzed by HPLC. (A) HPLC analysis of MEPTT-3 or BAMB-4 standards (B) HPLC analysis of methanol extracts from inhibitor-treated cells (C) HPLC analysis of methanol extracts from deficiency controls. Shown is one representative experiment out of three.

verify inhibition of InsP_3 kinase by EPPC-3, MEPTT-3 and BAMB-4, IC_{50} values were determined by an orthogonal assay, the coupled PK/LDH optical assay. This validation revealed that EPPC-3 did not inhibit InsP_3 kinase but luciferase activity. However, inhibition of InsP_3 kinase activity by MEPTT-3 and BAMB-4 could be reproduced by the coupled PK/LDH optical assay; the inhibitors showed IC_{50} values of $35 \pm 4 \mu\text{M}$ (MEPTT-3) and $20 \pm 3 \mu\text{M}$ (BAMB-4).

3.2. Cellular uptake of BAMB-4 and MEPTT-3

The chemical structure of MEPTT-3 and BAMB-4 indicates high membrane permeability. In order to validate this experimentally, uptake studies were performed. Lung cancer H1299 cells were

incubated with 100 μM MEPTT-3 or BAMB-4, respectively, over night. Afterwards, cells were extensively washed and compounds were extracted with methanol. For deficiency control, 100 μM of the compounds were added to trypsinized cell immediately prior to methanol extraction. The concentration of extracted substances was determined by HPLC. For MEPTT-3 a reverse phase C18 column was used, the compound was loaded with sodium dihydrogen phosphate (NaH_2PO_4) pH 2.8 (buffer A) and eluted with methanol (99%) (buffer B). BAMB-4 bound to a reverse phase C4-column in methanol- H_2O (1:10) (buffer A) and was eluted with acetonitrile/0.1% trifluoroacetic acid (buffer B). The MEPTT-3 standard eluted after 17.5 min at a 75% buffer B and showed one distinct peak while the BAMB-4 standard showed two peaks of which the first

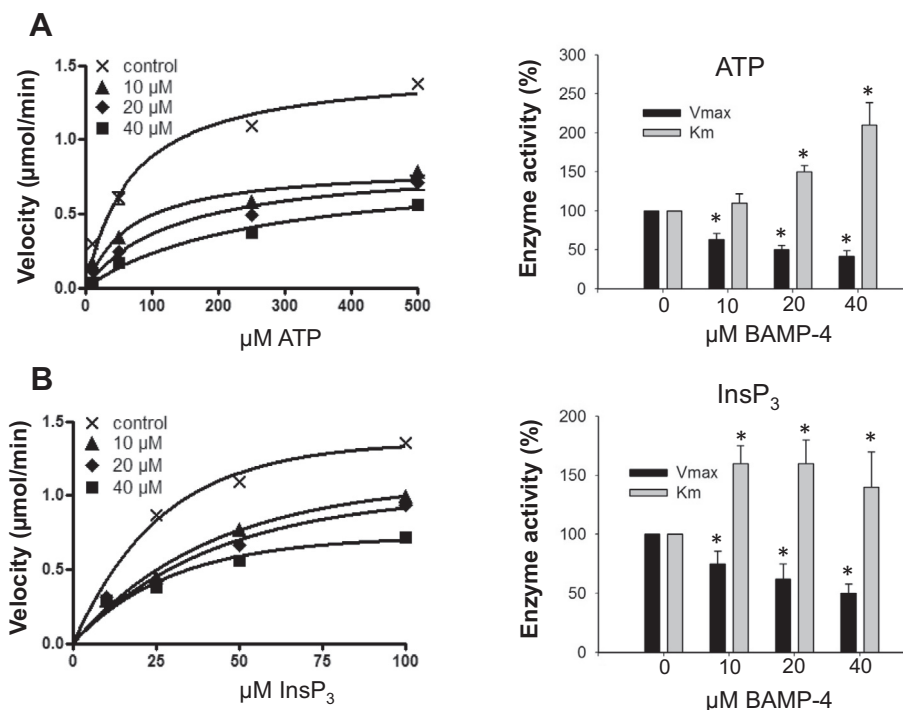


Fig. 3. Kinetic parameters of InsP₃kinase inhibitors. (A) Impact of BAMB-4 on V_{max} and K_m with respect to ATP. Enzyme activity was measured with 25 μM InsP₃ and varying ATP concentrations (10, 50, 250, 500 μM). (B) Impact of BAMB-4 on V_{max} and K_m with respect to InsP₃. Enzyme activity was measured with 500 μM ATP and varying InsP₃ concentrations 10, 25, 50, 100 μM. (A and B) For each measurement three different inhibitor concentrations (10, 20 and 40 μM) were applied. Left panels show saturation curves. In the right panels values for uninhibited enzyme were set to 100% and values for inhibited enzyme were calculated. Mean values \pm SD are shown. * $p < 0.001$ to $p < 0.0001$.

peak eluted at 50% buffer B after 13 min and the second peak at 70% buffer B after 19 min (Fig. 2A). According to the manufacturer (AKOS Consulting GmbH, Steinen, Germany) the two peaks of BAMB-4 result from the presence of an unsubstituted NH fragment, which is often ionized twice; ¹H NMR and ¹³C NMR analysis of BAMB-4 provided by AKOS are shown in Suppl. Figs. 2 and 3. In methanol extracts of cells incubated with MEPTT-3 no signal was detectable by HPLC (Fig. 2B, left panel) although methanol extracts of deficiency controls clearly shows that MEPTT-3 is extractable by methanol (Fig. 2C, left panel). Since MEPTT-3 has a hydrophobic structure we assume that the cells did have taken up the substance and degraded it immediately after uptake. This conclusion is primarily based on the result that after addition of MEPTT-3 to trypsinized H1299 cells (deficiency control) a strong degradation was visible (see Fig. 2C, left panel). On the other hand, 85 μM of 100 μM BAMB-4 added to the cell culture medium were detectable by HPLC. As we measured about a 20% loss after extraction procedure, BAMB-4 seems to be completely absorbed by the cells.

To our knowledge this is the first InsP₃kinase inhibitor which is completely absorbed by tumor cells and remains stable after cellular uptake. This property is essential to inhibit InsP₃kinase activity *in vivo* because even very potent inhibitors are not sufficient for application as long as they are not membrane permeable or are metabolized immediately after cellular uptake. In addition, BAMB-4 exhibit the lowest inhibition frequency among the InsP₃-Kinase inhibitors (see Table 2); only in one from 42 targets tested, BAMB-4 showed an inhibitory effect. Noteworthy, in kinase screens no targets of BAMB-4 were detected, indicating that the compound does not belong to the typical kinase inhibitors. Thus, the relative high specificity and the high cellular uptake of BAMB-4 now for the first provide the possibility to effectively inhibit InsP₃kinase *in vivo*.

3.3. Inhibition mechanism of BAMB-4

In a next step, we determined the inhibition type of BAMB-4 to examine which of the InsP₃Kinase substrates are affected by BAMB-4. There are two main types of enzyme inhibition: In case of competitive inhibition, the inhibitor and substrate compete for the active binding site of the enzyme resulting in an increase of K_m and no change in V_{max} . The non-competitive inhibition type is characterized by a decrease in V_{max} and no change of K_m because the inhibitor binds to an allosteric binding site which results in conformational change of the active binding site. The consequence is a reduction in enzymatic activity, but the inhibitor does not directly affect substrate binding. A mixed inhibition is a mixture of competitive and non-competitive inhibition; in presence of inhibitor V_{max} decreases and K_m increases [23–26].

In order to analyze the inhibition mechanism of BAMB-4, the effect of BAMB-4 on V_{max} and on K_m for both substrates of ITPKA, ATP and InsP₃, was measured as described in methods. The saturation curves of these measurements are depicted in Fig. 3A, B, left panel. To compare K_m and V_{max} of uninhibited with inhibited enzyme, values of uninhibited enzyme were set to 100% (Fig. 3 A, B, right panels). Our data show that BAMB-4 reduced V_{max} and increased K_m with respect to ATP and InsP₃. The K_m -value for ATP increased dose-dependent from 110% to 210% and V_{max} decreased from 62% to 42% as compared to non-treated enzyme. The K_m -value for InsP₃ increased at the lowest BAMB-4 concentration (10 μM) by 160% and did not further rise with elevated BAMB-4 concentrations, while V_{max} decreased dose-dependent from 75% to 50%. Our data showing increased K_m and decreased V_{max} in presence of inhibitor points to a mixed type inhibition.

In order to verify the proposed inhibition type for BAMB-4, the data depicted in Fig. 3 were analyzed by Lineweaver Burk- and Dixon-Plots. If in Lineweaver Burk-Plots the Y-intercepts between

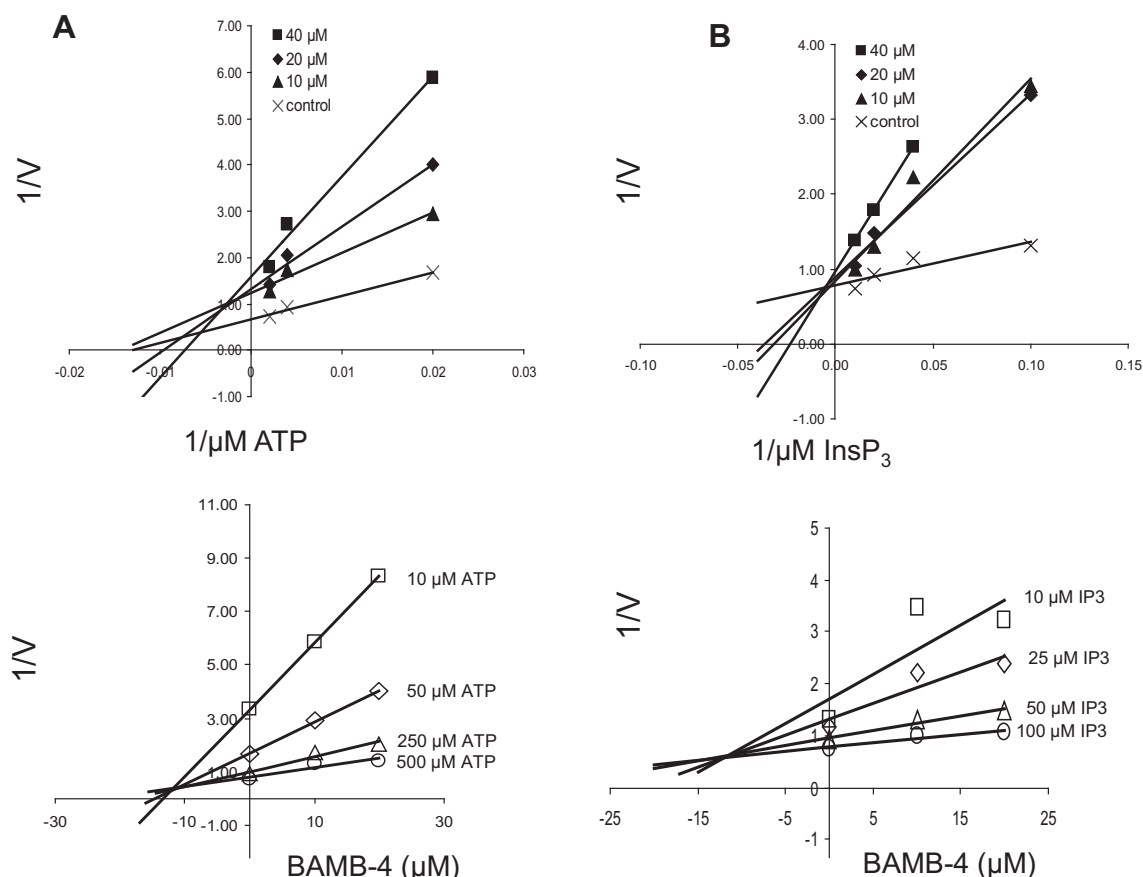


Fig. 4. Determination of inhibitor type of InsP_3 kinase inhibitors. (A) Upper panel: Lineweaver Burk Plot; ATP concentrations were varied and InsP_3 concentration was fixed. Reciprocal values of V_{\max} ($1/V$) are plotted against reciprocal ATP concentrations. Lower panel: Dixon Plot; reciprocal values of V_{\max} ($1/V$) are plotted against BAMB-4 concentrations. (B) Upper panel: Lineweaver Burk Plot; InsP_3 concentrations were varied and ATP concentration was fixed. Reciprocal values of V_{\max} ($1/V$) are plotted against reciprocal InsP_3 concentrations. Lower panel: Dixon Plot; reciprocal values of V_{\max} ($1/V$) are plotted against BAMB-4 concentrations.

lines resulting from data of inhibited and uninhibited enzyme are the same, the inhibitor is competitive. In case of non-competitive inhibitors, x-intercepts between inhibited and uninhibited sample are equal. In Lineweaver Burk as well as in Dixon Plots a mixed type inhibition is indicated when the intercepts of uninhibited and inhibited lines are located between the x- and y-axis in the second quadrant. Based on these considerations our data depicted in Fig. 4 confirm our conclusion that BAMB-4 is a mixed type inhibitor with respect to ATP and InsP_3 . The result that BAMB-4 does not only affect binding of ATP but also binding of InsP_3 is an important characteristic for a kinase inhibitor because pure ATP competitors mostly inhibit multiple cellular kinases due to the conserved ATP binding site, the DFG motif [15]. Thus, inhibitors which affect turnover of two substrate exhibit a higher inhibition specificity.

3.4. Conclusion

In this study a new inhibitor directed against the InsP_3 Kinase activity of ITPKA has been identified. This compound BAMB-4 is characterized by a relative high selectivity and a very high membrane permeability enabling inhibition of cellular InsP_3 Kinase activity. Thus, for the first time a relative specific membrane permeable inhibitor against the InsP_3 Kinase activity of ITPKA is available. As we recently demonstrated that the InsP_3 Kinase activity is essentially involved in ITPKA promoted metastasis of lung cancer cells, BAMB-4 is a promising therapeutic approach in lung cancer therapy. In future studies we will screen for inhibitors against the actin bundling activity of ITPKA to effectively inhibit the stimulating effect of ITPKA on metastasis of lung cancer.

Acknowledgements

We thank G. W. Mayr for helpful discussions concerning enzyme kinetic and Torsten Wundenberg for assistance in evaluation of K_m values by GraphPadPrism. We thank Christine Blechner and Werner Fanick for excellent technical assistance. In addition we are grateful to Edgar Specker for validating the inhibitory potential of compounds. We acknowledge the Deutsche Krebshilfe for funding this project (110873).

Appendix A. Supplementary data

Supplementary data associated with this article can be found, in the online version, at <http://dx.doi.org/10.1016/j.bbrc.2013.08.053>.

References

- [1] R. Siegel, D. Naishad, A. Jemal, Cancer statistics, *Can. J. Clin.* 62 (2012) 10–29.
- [2] C.L. Chaffer, R.A. Weinberg, A perspective on cancer cell metastasis, *Science* 331 (2011) 1559–1564.
- [3] A. Nürnberg, T. Kitzing, R. Grosse, Nucleating actin for invasion, *Nat. Rev. Cancer* 11 (2011) 177–187.
- [4] S. Windhorst, R. Fiegert, C. Blechner, K.M. Ilmann, Z. Hosseini, T. Günther, M. Eiben, L. Chang, H. Lin, W. Fanick, U. Schumacher, B. Brandt, G.W. Mayr, Inositol 1,4,5-Trisphosphate 3-kinase-A Is a new cell motility-promoting protein that increases the metastatic potential of tumor cells by two functional activities, *J. Biol. Chem.* 8 (2009) 5541–5554.
- [5] S. Windhorst, T. Kalinina, K. Schmid, C. Blechner, N. Kriebitzsch, R. Hinsch, L. Chang, L. Herich, U. Schumacher, G.W. Mayr, Functional role of inositol-1,4,5-trisphosphate-3-kinase-A for motility of malignant transformed cells, *Int. J. Cancer* 129 (2011) 1300–1309.

- [6] M.J. Schell, C. Erneux, R.F. Irvine, Inositol 1,4,5-trisphosphate 3-kinase A associates with F-actin and dendritic spines via its N terminus, *J. Biol. Chem.* 10 (2011) 37537–37546.
- [7] C.L. Clainche, M.F. Carlier, Regulation of actin assembly associated with protrusion and adhesion in cell migration, *Physiol. Rev.* 88 (2008) 489–513.
- [8] H.W. Davis, D.L. Crimmins, R.S. Thoma, J.G.N. Garcia, Phosphorylation of calmodulin in the first calcium binding, *Arch. Biochem. Biophys.* 1 (1996) 101–109.
- [9] C. Sutherland, M.P. Walsh, Myosin regulatory light chain diphosphorylation slows relaxation of arterial smooth muscle, *J. Biol. Chem.* 29 (2012) 24064–24076.
- [10] G.H. Li, P.D. Arora, Y. Chen, C.A. McCulloch, P. Liu, Multifunctional roles of gelsolin in health and diseases, *Med. Res. Rev.* 5 (2012) 999–1025.
- [11] V. Vanweyenberg, D. Communi, C.S. D'Santos, C. Erneux, Tissue- and cell-specific expression of Ins(1,4,5)P₃ 3-kinase isoenzymes, *Biochem. J.* 306 (1995) 429–435.
- [12] P. Mailleux, K. Takazawa, C. Erneux, J.J. Vanderhaeghen, Distributions of the neurons containing inositol 1,4,5-trisphosphate 3-kinase and its messenger RNA in the developing rat brain, *J. Comp. Neurol.* 327 (1993) 618–629.
- [13] G.W. Mayr, S. Windhorst, K. Hillemeier, Antiproliferative plant and synthetic polyphenolics are specific inhibitors of vertebrate Inositol-1,4,5-trisphosphate 3-kinases and inositol polyphosphate multikinase, *J. Biol. Chem.* 14 (2005) 13229–13240.
- [14] Y.T. Chang, G. Choi, Y.S. Bae, M. Burdett, H.S. Moon, J.W. Lee, N.S. Gray, P.G. Schultz, L. Meijer, S.K. Chung, K.Y. Choi, P.G. Suh, S.H. Ryu, Purine-based inhibitors of inositol-1,4,5-trisphosphate-3-kinase, *ChemBioChem* 9 (2002) 897–901.
- [15] L. Garuti, M. Roberti, G. Bottegoni, Non-ATP competitive protein kinase inhibitors, *Curr. Med. Chem.* 25 (2010) 2804–2821.
- [16] X. Cai, Z. Fang, J. Dou, A. Yu, G. Zhai, Bioavailability of quercetin: problems and promises, *Curr. Med. Chem.* 20 (2013) 2572–2582.
- [17] U. Bertsch, M. Haefs, M. Möller, C. Deschermeier, W. Fanick, A. Kitzerow, S. Ozaki, H.E. Meyer, G.W. Mayr, A novel A-isoform-like inositol 1,4,5-trisphosphate 3-kinase from chicken erythrocytes exhibits alternative splicing and conservation of intron positions between vertebrates and invertebrates, *Gene* 228 (1999) 61–71.
- [18] K. Koresawa, T. Okabe, High-throughput screening with quantitation of ATP consumption: a universal non-radioisotope, homogeneous assay for protein kinase, *Assay Drug Dev. Technol.* 2 (2004) 153–160.
- [19] T. Schröder, D. Minond, A. Weiser, C. Dao, J. Habel, T. Spicer, P. Chase, P. Baillargeon, L. Scampavia, S. Schürer, C. Chung, C. Mader, M. Southern, N. Tsinoremas, P. Lograsso, P. Hodder, Comparison of miniaturized time-resolved fluorescence resonance energy transfer and enzyme-coupled luciferase high-throughput screening assays to discover inhibitors of rho-kinase II (ROCK-II), *J. Biomol. Screen.* 13 (2008) 17–28.
- [20] H. Zegzouti, M. Zdanovskaia, K. Hsiao, S.A. Goueli, ADP-Glo: a bioluminescent and homogeneous ADP monitoring assay for kinases, *Assay Drug Technol.* 6 (2009) 560–572.
- [21] C. Brideau, B. Gunter, B. Pikounis, A. Liaw, Improved statistical methods for hit selection in high-throughput screening, *J. Biomol. Screen.* 8 (2003) 634–647.
- [22] J. Zhang, T.D. Chung, K.R. Oldenburg, A simple statistical parameter for use in evaluation and validation of high-throughput screening assays, *J. Biomol. Screen.* 4 (1999) 67–73.
- [23] L.B. Pearce, J.A. Roth, human brain monoamine oxidase type B: mechanism of deamination as probed by steady state methods, *J. Biochem.* 8 (1985) 1821–1826.
- [24] T. Efthimia, K. Leonardi, M.S. Azmitia, E.C. Azmitia, MDMA (ecstasy) inhibition of MAO type A and Type B: comparisons with fenfluramine and fluoxetine (Prozac), *Neuropsychopharmacology* 4 (1994) 231–238.
- [25] M. Gruno, P. Våljamäe, G. Pettersson, G. Johansson, Inhibition of the trichoderma reesei cellulase by cellobiose is strongly dependent on the nature of the substrate, *Biotechnol. Bioeng.* 5 (2003) 503–511.
- [26] S.J. Yin, Y.X. Si, G.Y. Qian, Inhibitory effect of phthalic acid on tyrosinase: the mixed-type inhibition and docking simulations, *Enzyme Res.* (2011) 1–7.